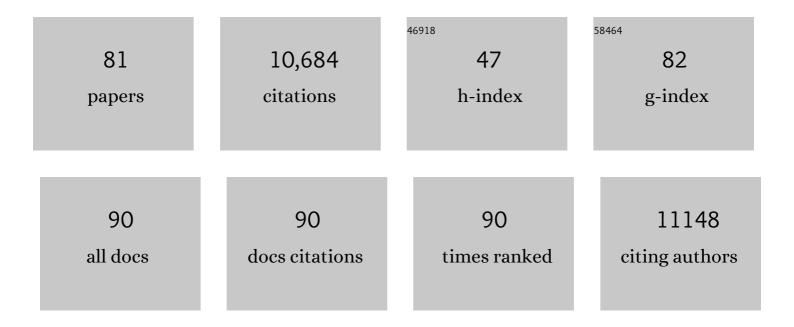
Helen R Saibil

List of Publications by Year in descending order

Source: https://exaly.com/author-pdf/3480786/publications.pdf Version: 2024-02-01



#	Article	lF	CITATIONS
1	Cryo-EM in molecular and cellular biology. Molecular Cell, 2022, 82, 274-284.	4.5	49
2	The pore conformation of lymphocyte perforin. Science Advances, 2022, 8, eabk3147.	4.7	10
3	Cooperative amyloid fibre binding and disassembly by the Hsp70 disaggregase. EMBO Journal, 2022, 41, .	3.5	14
4	2.7 à cryo-EM structure of ex vivo RML prion fibrils. Nature Communications, 2022, 13, .	5.8	66
5	The PDB and protein homeostasis: From chaperones to degradation and disaggregase machines. Journal of Biological Chemistry, 2021, 296, 100744.	1.6	9
6	Malaria Parasite Schizont Egress Antigen-1 Plays an Essential Role in Nuclear Segregation during Schizogony. MBio, 2021, 12, .	1.8	17
7	Correlative light and electron microscopy suggests that mutant huntingtin dysregulates the endolysosomal pathway in presymptomatic Huntington's disease. Acta Neuropathologica Communications, 2021, 9, 70.	2.4	7
8	REMBI: Recommended Metadata for Biological Images—enabling reuse of microscopy data in biology. Nature Methods, 2021, 18, 1418-1422.	9.0	63
9	Structural features distinguishing infectious ex vivo mammalian prions from non-infectious fibrillar assemblies generated in vitro. Scientific Reports, 2019, 9, 376.	1.6	37
10	Two-Step Activation Mechanism of the ClpB Disaggregase for Sequential Substrate Threading by the Main ATPase Motor. Cell Reports, 2019, 27, 3433-3446.e4.	2.9	46
11	Cryo-EM of amyloid fibrils and cellular aggregates. Current Opinion in Structural Biology, 2019, 58, 34-42.	2.6	112
12	A protease cascade regulates release of the human malaria parasite Plasmodium falciparum from host red blood cells. Nature Microbiology, 2018, 3, 447-455.	5.9	96
13	Perforin proteostasis is regulated through its C2 domain: supra-physiological cell death mediated by T431D-perforin. Cell Death and Differentiation, 2018, 25, 1517-1529.	5.0	4
14	A Liquid to Solid Phase Transition Underlying Pathological Huntingtin Exon1 Aggregation. Molecular Cell, 2018, 70, 588-601.e6.	4.5	252
15	A two-domain folding intermediate of RuBisCO in complex with the GroEL chaperonin. International Journal of Biological Macromolecules, 2018, 118, 671-675.	3.6	11
16	Real-time visualization of perforin nanopore assembly. Nature Nanotechnology, 2017, 12, 467-473.	15.6	88
17	Parasitophorous vacuole poration precedes its rupture and rapid host erythrocyte cytoskeleton collapse in <i>Plasmodium falciparum</i> egress. Proceedings of the National Academy of Sciences of the United States of America, 2017, 114, 3439-3444.	3.3	84
18	Structural pathway of regulated substrate transfer and threading through an Hsp100 disaggregase. Science Advances, 2017, 3, e1701726.	4.7	112

#	Article	IF	CITATIONS
19	Electron Bio-Imaging Centre (eBIC): the UK national research facility for biological electron microscopy. Acta Crystallographica Section D: Structural Biology, 2017, 73, 488-495.	1.1	24
20	The membrane attack complex, perforin and cholesterol-dependent cytolysin superfamily of pore-forming proteins. Journal of Cell Science, 2016, 129, 2125-33.	1.2	45
21	Structure of the poly-C9 component of the complement membrane attack complex. Nature Communications, 2016, 7, 10588.	5.8	112
22	<i>Ex vivo</i> mammalian prions are formed of paired double helical prion protein fibrils. Open Biology, 2016, 6, 160035.	1.5	55
23	Atomic force microscopy of membrane pore formation by cholesterol dependent cytolysins. Current Opinion in Structural Biology, 2016, 39, 8-15.	2.6	17
24	Cryo electron microscopy to determine the structure of macromolecular complexes. Methods, 2016, 95, 78-85.	1.9	82
25	A novel and rapid method for obtaining high titre intact prion strains from mammalian brain. Scientific Reports, 2015, 5, 10062.	1.6	51
26	Structure of a bacterial type III secretion system in contact with a host membrane in situ. Nature Communications, 2015, 6, 10114.	5.8	92
27	A national facility for biological cryo-electron microscopy. Acta Crystallographica Section D: Biological Crystallography, 2015, 71, 127-135.	2.5	22
28	Outcome of the First wwPDB Hybrid/Integrative Methods Task Force Workshop. Structure, 2015, 23, 1156-1167.	1.6	159
29	Conformational Changes during Pore Formation by the Perforin-Related Protein Pleurotolysin. PLoS Biology, 2015, 13, e1002049.	2.6	114
30	Processing of Plasmodium falciparum Merozoite Surface Protein MSP1 Activates a Spectrin-Binding Function Enabling Parasite Egress from RBCs. Cell Host and Microbe, 2015, 18, 433-444.	5.1	141
31	Prion aggregate structure in yeast cells is determined by the Hsp104-Hsp110 disaggregase machinery. Journal of Cell Biology, 2015, 211, 145-158.	2.3	28
32	Human Hsp70 Disaggregase Reverses Parkinson's-Linked α-Synuclein Amyloid Fibrils. Molecular Cell, 2015, 59, 781-793.	4.5	336
33	Making connections: snapshots of chlamydial type III secretion systems in contact with host membranes. Current Opinion in Microbiology, 2015, 23, 1-7.	2.3	12
34	N-terminal Domain of Prion Protein Directs Its Oligomeric Association. Journal of Biological Chemistry, 2014, 289, 25497-25508.	1.6	20
35	A 3D cellular context for the macromolecular world. Nature Structural and Molecular Biology, 2014, 21, 841-845.	3.6	47
36	Head-to-tail interactions of the coiled-coil domains regulate ClpB activity and cooperation with Hsp70 in protein disaggregation. ELife, 2014, 3, e02481.	2.8	111

#	Article	IF	CITATIONS
37	Stepwise visualization of membrane pore formation by suilysin, a bacterial cholesterol-dependent cytolysin. ELife, 2014, 3, e04247.	2.8	145
38	ATPâ€driven molecular chaperone machines. Biopolymers, 2013, 99, 846-859.	1.2	76
39	Atomic structure and hierarchical assembly of a cross-β amyloid fibril. Proceedings of the National Academy of Sciences of the United States of America, 2013, 110, 5468-5473.	3.3	479
40	Chaperone machines for protein folding, unfolding and disaggregation. Nature Reviews Molecular Cell Biology, 2013, 14, 630-642.	16.1	836
41	Structure and Allostery of the Chaperonin GroEL. Journal of Molecular Biology, 2013, 425, 1476-1487.	2.0	153
42	Machinery to Reverse Irreversible Aggregates. Science, 2013, 339, 1040-1041.	6.0	11
43	Heritable yeast prions have a highly organized three-dimensional architecture with interfiber structures. Proceedings of the National Academy of Sciences of the United States of America, 2012, 109, 14906-14911.	3.3	38
44	Direct three-dimensional visualization of membrane disruption by amyloid fibrils. Proceedings of the National Academy of Sciences of the United States of America, 2012, 109, 20455-20460.	3.3	162
45	ATP-Triggered Conformational Changes Delineate Substrate-Binding and -Folding Mechanics of the GroEL Chaperonin. Cell, 2012, 149, 113-123.	13.5	160
46	The structural basis for membrane binding and pore formation by lymphocyte perforin. Nature, 2010, 468, 447-451.	13.7	364
47	Methods for Three-Dimensional Reconstruction of Heterogeneous Assemblies. Methods in Enzymology, 2010, 482, 321-341.	0.4	38
48	Separating and visualising protein assemblies by means of preparative mass spectrometry and microscopy. Journal of Structural Biology, 2010, 172, 161-168.	1.3	64
49	Cryo electron microscopy structures of Hsp100 proteins: crowbars in or out?This paper is one of a selection of papers published in this special issue entitled 8th International Conference on AAA Proteins and has undergone the Journal's usual peer review process Biochemistry and Cell Biology, 2010. 88. 89-96.	0.9	19
50	Macromolecular assemblies. Current Opinion in Structural Biology, 2009, 19, 178-180.	2.6	0
51	The Molecular Basis for Perforin Oligomerization and Transmembrane Pore Assembly. Immunity, 2009, 30, 684-695.	6.6	123
52	Motor Mechanism for Protein Threading through Hsp104. Molecular Cell, 2009, 34, 81-92.	4.5	84
53	Chaperone machines in action. Current Opinion in Structural Biology, 2008, 18, 35-42.	2.6	147
54	Multiple States of a Nucleotide-Bound Group 2 Chaperonin. Structure, 2008, 16, 528-534.	1.6	32

#	Article	IF	CITATIONS
55	Detection and separation of heterogeneity in molecular complexes by statistical analysis of their two-dimensional projections. Journal of Structural Biology, 2008, 162, 108-120.	1.3	75
56	Atypical AAA+ Subunit Packing Creates an Expanded Cavity for Disaggregation by the Protein-Remodeling Factor Hsp104. Cell, 2007, 131, 1366-1377.	13.5	107
57	Topologies of a Substrate Protein Bound to the Chaperonin GroEL. Molecular Cell, 2007, 26, 415-426.	4.5	96
58	Allosteric signaling of ATP hydrolysis in GroEL–GroES complexes. Nature Structural and Molecular Biology, 2006, 13, 147-152.	3.6	142
59	Elongated Oligomers Assemble into Mammalian PrP Amyloid Fibrils. Journal of Molecular Biology, 2006, 357, 975-985.	2.0	61
60	An Expanded Protein Folding Cage in the GroEL–gp31 Complex. Journal of Molecular Biology, 2006, 358, 905-911.	2.0	26
61	Structure of an Hsp90-Cdc37-Cdk4 Complex. Molecular Cell, 2006, 23, 697-707.	4.5	288
62	Three-Dimensional Structural Analysis of Amyloid Fibrils by Electron Microscopy. , 2006, , 303-313.		2
63	The mechanism of pore formation by bacterial toxins. Current Opinion in Structural Biology, 2006, 16, 230-236.	2.6	132
64	Multiple Distinct Assemblies Reveal Conformational Flexibility in the Small Heat Shock Protein Hsp26. Structure, 2006, 14, 1197-1204.	1.6	87
65	Structural Basis of Pore Formation by the Bacterial Toxin Pneumolysin. Cell, 2005, 121, 247-256.	13.5	369
66	Folding with and without encapsulation by cis- and trans-only GroEL-GroES complexes. EMBO Journal, 2003, 22, 3220-3230.	3.5	70
67	The protofilament structure of insulin amyloid fibrils. Proceedings of the National Academy of Sciences of the United States of America, 2002, 99, 9196-9201.	3.3	770
68	ATP-Bound States of GroEL Captured by Cryo-Electron Microscopy. Cell, 2001, 107, 869-879.	13.5	274
69	Macromolecular structure determination by cryo-electron microscopy. Acta Crystallographica Section D: Biological Crystallography, 2000, 56, 1215-1222.	2.5	47
70	Conformational changes studied by cryo-electron microscopy. , 2000, 7, 711-714.		78
71	Three conformations of an archaeal chaperonin, TF55 from Sulfolobus shibatae. Journal of Molecular Biology, 2000, 296, 813-819.	2.0	74
72	Domain rotations between open, closed and bullet-shaped forms of the thermosome, an archaeal chaperonin 1 1Edited by A. R. Fersht. Journal of Molecular Biology, 2000, 301, 323-332.	2.0	56

#	Article	IF	CITATIONS
73	Structural basis of pore formation by cholesterol-binding toxins. International Journal of Medical Microbiology, 2000, 290, 389-394.	1.5	9
74	Multivalent Binding of Nonnative Substrate Proteins by the Chaperonin GroEL. Cell, 2000, 100, 561-573.	13.5	183
75	Cryo-electron microscopy structure of an SH3 amyloid fibril and model of the molecular packing. EMBO Journal, 1999, 18, 815-821.	3.5	487
76	GroEL-GroES Cycling. Cell, 1999, 97, 325-338.	13.5	308
77	Two Structural Transitions in Membrane Pore Formation by Pneumolysin, the Pore-Forming Toxin of Streptococcus pneumoniae. Cell, 1999, 97, 647-655.	13.5	174
78	The Chaperonin ATPase Cycle: Mechanism of Allosteric Switching and Movements of Substrate-Binding Domains in GroEL. Cell, 1996, 87, 241-251.	13.5	389
79	Mechanism of GroEL action: Productive release of polypeptide from a sequestered position under groes. Cell, 1995, 83, 577-587.	13.5	431
80	Subunit organisation and symmetry of pore-forming, oligomeric pneumolysin. FEBS Letters, 1995, 371, 77-80.	1.3	51
81	Location of a folding protein and shape changes in GroEL–GroES complexes imaged by cryo-electron microscopy. Nature, 1994, 371, 261-264.	13.7	366